

AperTO - Archivio Istituzionale Open Access dell'Università di Torino

Diamond and its olivine inclusions: a strange relation revealed by ab initio simulations.

This is a pre print version of the following article:

Original Citation:

Availability:

This version is available <http://hdl.handle.net/2318/1559538> since 2016-04-06T16:30:15Z

Published version:

DOI:10.1016/j.epsl.2015.12.011

Terms of use:

Open Access

Anyone can freely access the full text of works made available as "Open Access". Works made available under a Creative Commons license can be used according to the terms and conditions of said license. Use of all other works requires consent of the right holder (author or publisher) if not exempted from copyright protection by the applicable law.

(Article begins on next page)

1 **Diamond and its olivine inclusions: a strange relation revealed by ab initio**
2 **simulations**

3 M. Bruno^{1*}, M. Rubbo¹, D. Aquilano¹, F.R. Massaro² & F. Nestola²

4

5 ¹ Dipartimento di Scienze della Terra, Università degli Studi di Torino, Via Valperga Caluso 35, I-
6 10125 Torino, Italy

7 ² Dipartimento di Geoscienze, Università degli Studi di Padova, Via Gradenigo 6, I-35131 Padova,
8 Italy

9

10 *Corresponding author
11 Email: marco.bruno@unito.it
12 Tel: +39 011 6705126
13 Fax: +39 011 6705128

14

15 **Abstract**

16 The study of diamond and its solid inclusions is of paramount importance to acquire direct
17 information on the deepest regions of the Earth. However, although diamond is one of the most
18 studied materials in geology, the diamond-inclusion relationships are not yet understood: do they
19 form simultaneously (syngenesi) or are inclusions pre-existing objects on which diamond
20 nucleated (protogenesis)?

21 Here we report, for the first time, adhesion energies between diamond (D) and forsterite (Fo) to
22 provide a crucial contribution to the syngenesi/protogenesis debate. The following interfaces were
23 investigated at quantum-mechanical level: (i) (001)_D/(001)_{Fo}, (ii) (001)_D/(021)_{Fo}, and (iii)
24 (111)_D/(001)_{Fo}. Our data, along with the ones recently obtained on the (110)_D/(101)_{Fo} interface,
25 revealed an unexpected thermodynamic behaviour, all interfaces showing almost equal and low
26 adhesion energies: accordingly, diamond and olivine have an extremely low chemical affinity and
27 cannot develop preferential orientations, even during an eventual epitaxial growth. Combining these

28 results with those of our previous work concerning the morphology constraints of diamond on its
29 inclusions, we can state that the two main arguments used so far in favour of diamond/inclusions
30 syngeneses cannot be longer considered valid, at least for olivine.

31
32 **Key words:** diamond, olivine inclusion, epitaxy, syngeneses, protogeneses

34 1. Introduction

35 The characterization of mineral inclusions in diamond (D) allowed to indirectly obtain information
36 about the genesis and distribution of diamonds in the Earth's mantle (e.g., Pearson et al., 2014;
37 Shirey et al., 2013; Stachel and Harris, 2008). Such inclusions have been classified, according to the
38 timing of their formation with respect to the host diamond (Meyer, 1987; Harris, 1968a, 1968b), as:
39 (i) *syngenetic*: when they form simultaneously with the diamond; then, syngeneses implies either
40 inclusion/host mutual growth through co-precipitation from the same medium or complete
41 recrystallization of a pre-existing mineral occurring when diamond grows; (ii) *protogenetic*: when
42 they represent pre-existing minerals passively incorporated into the growing diamond; (iii)
43 *epigenetic*: when they are secondary minerals forming into a pre-existing diamond.

44 Determining whether an inclusion is syngenetic or protogenetic is of paramount importance
45 in diamond studies. Indeed, any geological information concerning a syngenetic inclusion (i.e.,
46 pressure and temperature of formation, age, geochemistry of the mother-medium) is applicable to
47 the host diamond: accordingly, a wrong interpretation concerning the genesis of the diamond-
48 inclusion couple could address to a misleading idea about the geological processes involved in the
49 diamond formation.

50 The most common proof invoked to establish if an inclusion is syngenetic lies in the
51 imposition of the morphology of the diamond on the inclusion (e.g., Sobolev, 1977; Harris, 1968a).
52 Such a traditional criterion is based on the belief that diamond can impose its cube-octahedral
53 morphology upon the inclusion only during their mutual growth. However, this is not supported by

54 any chemical-physical arguments, and even less by experimental evidences. Recently, the
55 morphologic criterion has been strongly criticized (Bruno et al., 2014; Nestola et al., 2014; Taylor
56 and Anand, 2004; Taylor et al., 2003). In particular, by analysing the diamond-imposed morphology
57 (Bruno et al., 2014) and the orientations (Nestola et al. 2014) of 43 olivine inclusions in 20
58 diamonds from the world-famous Udachnaya kimberlite in Siberia (Russia), the authors found that
59 many, if not most, olivine inclusions in diamonds are protogenetic and the diamond-imposed
60 morphology alone cannot be considered as a compelling proof of syngensis of mineral inclusions
61 in diamonds.

62 The identification of an epitaxy, on the base of the orientation of the inclusion with respect
63 to its host (Pearson and Shirey, 1999; Harris and Gurney, 1979; Orlov, 1977; Sobolev, 1977), has
64 been considered as a further proof of syngensis. Unfortunately, the only two works reporting a
65 statistically significant collection of data, have been recently published by Nestola et al. (2014) on
66 the Udachnaya diamonds and Neuser et al. (2015) on the Yubileinaya diamonds (Yakutia). In both
67 papers, the olivine inclusions were shown to be randomly oriented with respect to the hosting
68 diamond: Nestola et al. (2014) performed X-ray diffraction measurements, whereas Neuser et al.
69 (2015) carried out an EBSD analysis in order to determine the crystallographic orientations of the
70 inclusions. Previous works only reported limited sets of samples that are not sufficient to identify,
71 on a firm statistical ground, the mutual orientations between the crystallographic axes of the
72 inclusion and those of the host diamond (Frank-Kamenetsky, 1964; Futergendler and Frank-
73 Kamenetsky, 1961; Mitchell and Giardini, 1953). Moreover, the majority of these papers did not
74 consider the crystallographic contact planes (CCPs) defining the epitaxial interface. The latter
75 information is necessary to asses unambiguously a *preferential* epitaxial relationship since, on a
76 purely geometrical point of view, no constraints can be required on the contact plane of two
77 different phases with the same crystallographic orientation, the number of CCPs being potentially
78 infinite (Fig. S1, Supplementary Material). Indeed, if the inclusions do not show a systematic
79 preferential orientation with respect to diamond (random orientations), one is allowed to state that

80 there cannot be preferential epitaxial relationships, yet undefined. Conversely, the absence of
81 preferential orientation relationships is not sufficient to conclude that there is not an epitaxial
82 growth, as we will show in this work. Accordingly, it is evident that the *epitaxial criterion* to define
83 syngeneses can result rather ambiguous, if no information can be found on the thermodynamic
84 properties of the epitaxial interface.

85 Here, we focus on the study of the epitaxial phenomena in olivine-diamond system by an *ab*
86 *initio* quantum-mechanical computational approach, as such crystal features cannot be
87 experimentally investigated. Olivine forms a complete isomorphous series, with composition
88 ranging from forsterite (Mg_2SiO_4 , Fo) to fayalite (Fe_2SiO_4 , Fa). However, typical Earth's mantle
89 olivines are Mg-richer ($\text{Fo}_{92}\text{Fa}_8$) (e.g., Nestola et al., 2011). For this and for sake of simplicity, the
90 fayalite contribution in our model system was neglected. We investigated the $(001)_{\text{D}}/(001)_{\text{Fo}}$,
91 $(001)_{\text{D}}/(021)_{\text{Fo}}$, and $(111)_{\text{D}}/(001)_{\text{Fo}}$ epitaxial interfaces determining their structures and
92 thermodynamic properties. In detail, the specific adhesion energy $\beta_{(hkl)/(h'k'l')}^{D/\text{Fo}}$ (i.e., the energy gained,
93 per unit area, once the interface is formed) and the specific interface energy $\gamma_{(hkl)/(h'k'l')}^{D/\text{Fo}}$ (i.e., the
94 energy needed to create, per unit area, the interface), were calculated; (hkl) and $(h'k'l')$ define the
95 crystallographic faces in epitaxy of D and Fo, respectively. We decided to study the $(001)_{\text{D}}/(001)_{\text{Fo}}$,
96 $(001)_{\text{D}}/(021)_{\text{Fo}}$ and $(111)_{\text{D}}/(001)_{\text{Fo}}$ interfaces for two reasons: (i) the $(001)_{\text{D}}$, $(111)_{\text{D}}$, $(001)_{\text{Fo}}$ and
97 $(021)_{\text{Fo}}$ are important faces in the crystal morphology of diamond and olivine (e.g., Bruno et al.,
98 2014; De La Pierre et al., 2014); (ii) from a computational point of view, these systems are
99 workable with the resources of calculus actually in our hand.

100

101 **2. Calculation**

102 The calculations were performed with the *ab initio* CRYSTAL09 code (Dovesi et al., 2009; Dovesi
103 et al., 2005; Pisani et al., 1988) and at the DFT (Density Functional Theory) level with the B3LYP
104 Hamiltonian (Stephens et al., 1994; Becke, 1993; Lee et al., 1988), which provided accurate results
105 for the surface properties of the minerals considered in the present work (Bruno et al., 2014; De La

106 Pierre et al., 2014; Demichelis et al., 2015). Further computational details (e.g., basis set, thresholds
107 controlling the accuracy of the calculations) are given as Supplementary Material.

108 A composed slab (D/Fo/D), made by diamond (D) and forsterite (Fo) (slab D and slab Fo
109 hereinafter), was generated in the following way: (i) the two-dimensional (2D) coincidence lattices
110 between the two phases in epitaxial relationship were identified (Bruno et al. 2015); (ii) the slabs D
111 and Fo of a selected thickness were made by cutting their respective bulk structures parallel to the
112 *hkl* planes of interest and using the same 2D cell parameters describing the epitaxy; (iii) the slab Fo
113 was placed in between two slabs D; (iv) finally, the composed slab structure (atomic coordinates
114 and 2D cell parameters) was optimized by considering all the atoms free to move. The slab D/Fo/D
115 was generated preserving the symmetry centre, to ensure the vanishing of the dipole component
116 perpendicular to the slab. The CRYSTAL09 output files, listing the optimized fractional coordinates
117 and optimized 2D cell parameters of the composed slabs, are freely available at
118 <http://mabruno.weebly.com/download>. The calculations were performed by considering composed
119 slabs with a thickness sufficient to obtain an accurate description of the interfaces. The slab
120 thickness is considered appropriate when the bulk-like properties are reproduced at the centre of the
121 slabs D and Fo. Further details are given as Supplementary Material.

122 The specific adhesion energy, $\beta_{(hkl)/(h'k'l')}^{D/Fo}$ (J/m²), is calculated by means of the relation:

123

$$124 \quad \beta_{(hkl)/(h'k'l')}^{D/Fo} = \frac{E(2D) + E(Fo) - E(2D + Fo)}{2S} \quad (1)$$

125

126 where E(2D+Fo), E(2D) and E(Fo) are the static energies at 0K of the optimized slab D/Fo/D, slab
127 D/vacuum/D and slab Fo, respectively, and *S* is the area of the surface unit cell. Accordingly, the
128 surface energy is calculated:

129

$$130 \quad \gamma_{(hkl)}^i = \frac{E(i) - E_b(i)}{2S}; i = D, Fo \quad (2)$$

131

132 where $E_b(i)$ is the bulk energy of the i -th phase and the factor of 2 in the denominator accounts for
133 the upper and lower surfaces of the slab model.

134

135 **3. Results and discussion**

136 In Fig.1, the optimized structure of the $(001)_D/(001)_{Fo}$ interface is reported; the $(111)_D/(001)_{Fo}$ and
137 $(001)_D/(021)_{Fo}$ interfaces are given in Figs. S2 and S3 (Supplementary Material). A detailed
138 structural analysis of the interfaces is out of the scope of this work, therefore only a qualitative and
139 short description is given in the following. People interested to an in-depth structural analysis can
140 carry out it by using the CRYSTAL09 output file reporting the optimized atomic coordinates.

141 The significant structural modifications we observe at the three interfaces are not due to a strong
142 *chemical* interaction between the two phases, as it ensues from the comparison of the relaxed
143 structures of the surfaces in contact both with vacuum and the other mineral (Fig. 1 and Figs. S2-
144 S4). Indeed, the relaxation of the $(001)_D$ and $(111)_D$ surfaces in vacuum (De La Pierre et al., 2014)
145 only slightly differs from that observed when they are in contact with the (001) and (021) faces of
146 forsterite. To describe this geometry modification, we define the roughness of the carbon layer at
147 the interface with the parameter Δz (i.e., the difference between the z coordinates of the carbon
148 atoms within the same layer). Δz is 0.0206 Å for the carbon layer of the $(001)_D$ surface in vacuum,
149 whereas Δz is 0.2144 Å and 0.1712 Å for the carbon layer in contact with $(001)_{Fo}$ and $(021)_{Fo}$,
150 respectively. An analogous relaxation was reported by Bruno et al. (2015) for the $(110)_D$ surface: Δz
151 = 0.0038 Å for the carbon layer in vacuum and $\Delta z = 0.1966$ Å for the one in contact with $(101)_{Fo}$.
152 For the $(111)_D$ surface, the relaxation is smaller: $\Delta z = 0.0028$ and $\Delta z = 0.0298$ Å for that in vacuum
153 and in contact with $(001)_{Fo}$, respectively.

154 Similarly, the $(001)_{Fo}$ and $(021)_{Fo}$ surfaces are slightly affected by the presence of the diamond. The
155 strong distortion of the SiO_4 tetrahedra in proximity of the outmost diamond surfaces is analogue to
156 that found for the surface in vacuum. Majors differences are due to the distortion and rotation of

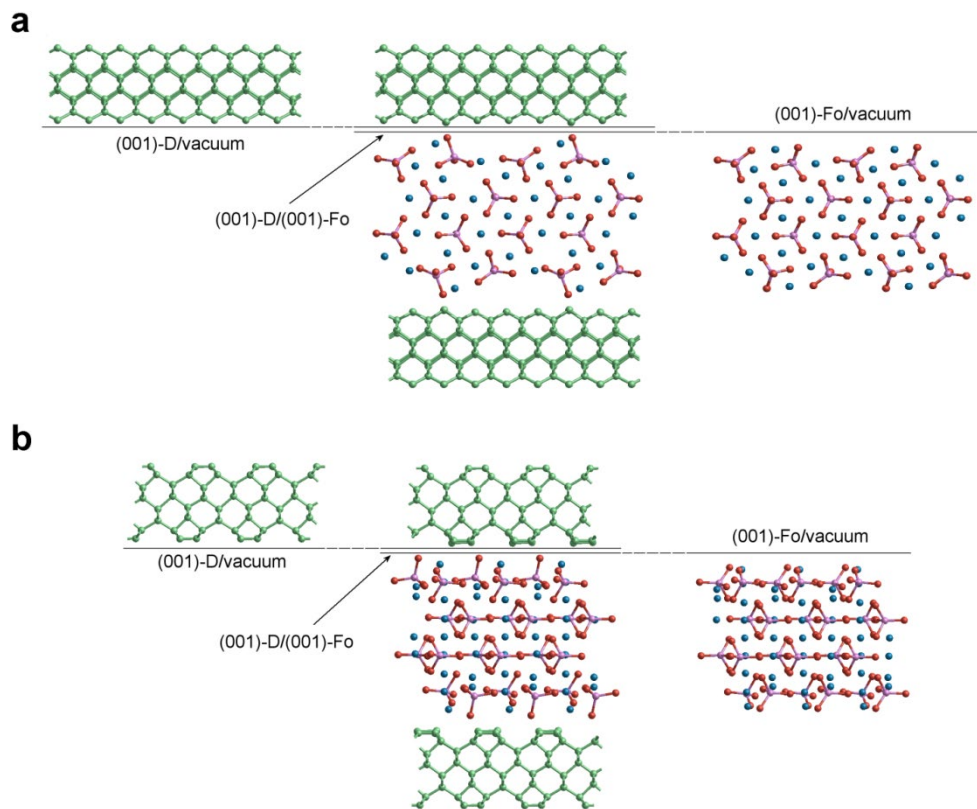
157 some SiO₄ tetrahedra to form C–O bonds in the (001)_D/(001)_{Fo} and (110)_D/(101)_{Fo} (Bruno et al.,
 158 2015) interfaces.

159

160 **Table 1.** Optimized 2D cell parameters, adhesion and interfacial energies for the diamond/forsterite
 161 epitaxies. The interfacial energies are calculated through Dupré’s relation (e.g., Mutaftschiev, 2001)
 162 and the following surface energy values: $\gamma_{(001)}^D = 4.820$, $\gamma_{(111)}^D = 3.849$, $\gamma_{(110)}^D = 5.046$, $\gamma_{(001)}^{Fo} = 1.676$,
 163 $\gamma_{(021)}^{Fo} = 1.900$ and $\gamma_{(101)}^{Fo} = 1.696$ J/m². The data for the (110)_D/(101)_{Fo} interface are from Bruno et al.
 164 (2015).

interface	atoms	a (Å)	b (Å)	a^b (°)	area (Å ²)	β (J/m ²)	γ (J/m ²)
(001) _D /(001) _{Fo}	184	10.2382	4.9614	89.67	50.80	0.391	6.105
(111) _D /(001) _{Fo}	184	4.9899	9.9466	119.79	43.07	-0.934	6.459
(001) _D /(021) _{Fo}	304	4.9486	15.4411	89.95	76.41	0.243	6.477
(110) _D /(101) _{Fo}	280	7.4210	10.0444	90.09	74.54	0.367	6.375

165



166

167 **Fig. 1.** Optimized (001)_D/(001)_{Fo} (middle), (001)_D/vacuum (left) and (001)_{Fo}/vacuum interfaces
 168 (right). The slabs are viewed along the (a) [110] and (b) [1 $\bar{1}$ 0] directions of diamond. Mg, Si, O,
 169 and C are blue, pink, red, and green, respectively. The black lines are a guide for eyes to indicate the
 170 interfaces.

171

172 The weak interaction localized at the D/Fo interface can be ascribed to the extreme rigidity
173 of the diamond surfaces and to the noteworthy difference between the crystal fields belonging to the
174 two phases. Such structural incompatibility generates very low and similar values of the adhesion
175 energy (Table 1) for the $(001)_D/(001)_{Fo}$, $(001)_D/(021)_{Fo}$ and $(110)_D/(101)_{Fo}$ (Bruno et al., 2015)
176 interfaces, 0.243-0.391 J/m² (differences are within the calculation accuracy), and even a negative
177 one for the $(111)_D/(001)_{Fo}$ interface, -0.934 J/m². Interestingly, different values of $\beta_{(hkl)/(h'k'l')}^{D/Fo}$ provide
178 very similar values of $\gamma_{(hkl)/(h'k'l')}^{D/Fo}$ (Table 1) when the Dupré's relation (e.g., Mutaftschiev, 2001) is
179 used ($\gamma_{(hkl)/(h'k'l')}^{D/Fo} = \gamma_{(hkl)}^D + \gamma_{(h'k'l')}^{Fo} - \beta_{(hkl)/(h'k'l')}^{D/Fo}$), where $\gamma_{(hkl)}^D$ and $\gamma_{(h'k'l')}^{Fo}$ are the surface energies in the
180 vacuum of diamond and forsterite): 6.105-6.477 J/m². The implications of these findings are
181 numerous and outstanding. The epitaxy between the (111) face of diamond and forsterite results to
182 be very likely impossible. However, further calculations on epitaxial systems involving the $(111)_D$
183 and other forsterite surfaces could be performed to verify this statement. The (110) and (001) faces
184 of diamond show an undifferentiated behaviour with regard to forsterite; they seem to have the
185 same probability to make epitaxy with whatever surface of forsterite. According to the classical
186 nucleation theory (e.g., Mutaftschiev, 2001), lower the adhesion energy, lower the probability of the
187 3D-heterogeneous nucleation to occur (i.e., the formation of 3D nuclei of a phase A above a phase
188 B), the 3D-homogeneous nucleation becoming competitive as much as $\beta_{(hkl)/(h'k'l')}^{D/Fo}$ approaches to
189 zero. When $\beta_{(hkl)/(h'k'l')}^{D/Fo}$ is negative, as for the $(111)_D/(001)_{Fo}$ interface, a very peculiar case is spotted:
190 the homogeneous nucleation could occur more likely than the heterogeneous one.

191 An extremely interesting consequence of our calculations concerns the impossibility of the
192 diamond-forsterite system to develop a preferential orientation during any possible epitaxial growth.
193 This is in agreement with the recent crystallographic observations reported by Nestola et al. (2014)
194 and Neuser et al. (2015), where no overall preferred orientation of olivines in diamond was found. It
195 is evident that our results cast serious doubts on the application of the mere crystallographic

196 measurements of the relative orientations of diamond and olivine inclusions to hypothesize epitaxy
197 and, eventually, syngeneses. Indeed, if a preferential crystallographic orientation between inclusion
198 and host is not observed, this does not mean that the epitaxy cannot be realized; on the contrary,
199 epitaxy could occur through several D/Fo interfaces owing to the quasi-invariance of their adhesion
200 energy. Other silicate inclusions in diamond, with their outmost surfaces exhibiting SiO₄ tetrahedra,
201 like olivine, could show analogous behaviour. Preliminary measurements on orientation of garnet
202 inclusion in diamond (F. Nestola, personal communication), where a random distribution is
203 observed, seem to confirm such assumption.

204 Finally, from our findings on the quasi-invariance of the adhesion energies, the *epitaxial*
205 *criterion* alone results to be not adequate to discriminate between syngeneses and protogeneses in
206 the case of diamond-olivine pair. Three scenarios can be depicted to explain this concept. First, we
207 suppose a protogenetic origin for olivine: diamonds form from a carbon-rich fluid or melt
208 percolating homogeneously through an olivine-rich mantle rock (i.e., peridotite), by nucleating and
209 growing indifferently onto any olivine surfaces. Then, diamonds continue growing and fragments of
210 pre-existing olivine are entrapped. This represents a highly favorable scenario, since the mantle
211 rock is mainly composed by olivine and heterogeneous nucleation is always favored with respect to
212 the homogeneous one when $\beta_{(hkl)/(h'k'l')}^{D/Fo}$ is positive. Such a path should generate a rock containing
213 randomly oriented diamonds.

214 The second scenario accounts for a syngenetic origin of olivine inclusions: diamond nucleates
215 somewhere within the rock and, at a certain point of its history, olivines nucleate and grow on
216 diamond surfaces during its ongoing growth, without developing a preferential epitaxial
217 relationship, due to the quasi-invariance of $\beta_{(hkl)/(h'k'l')}^{D/Fo}$ values. Then, as for the protogenetic case, the
218 new formed olivines are entrapped in the growing diamonds without any preferential orientation.

219 In the last scenario, diamonds and olivines form through a homogeneous nucleation in the fluid.
220 Without an epitaxial control, no preferential crystallographic orientation can be developed: also in
221 this case, a rock having diamonds and its olivine inclusions with random orientations should be

222 obtained.

223 Summing up, no overall preferred orientation of olivines in diamond can be identified in a mantle
224 rock, both for syngensis and protogenesis, as well as both in the case of heterogeneous and
225 homogeneous nucleation. Combining our results with those of Bruno et al. (2014) concerning the
226 morphology imposition by diamond on its inclusions, we can state that the two main arguments
227 playing in favour of syngensis between diamond and its inclusions cannot be longer considered
228 valid. Alternative explanations must be provided to demonstrate the growth relationship between
229 diamond and its inclusions.

230

231 **4. Conclusions**

232 In this work, both the structure and energetics of the $(001)_D/(001)_{Fo}$, $(001)_D/(021)_{Fo}$, and
233 $(111)_D/(001)_{Fo}$ epitaxial interfaces were determined for the first time by means of *ab initio* quantum-
234 mechanical simulations. Our results can be summarized as follow:

235 (i) Diamond and forsterite have an extremely low chemical affinity: all interfaces show almost
236 equal and low adhesion energies.

237 (ii) From our findings on the quasi-invariance of the adhesion energies we can state that the
238 diamond-forsterite system is not able to develop a preferential orientation during any possible
239 epitaxial growth. Then, no overall preferred orientation of olivines in diamond can be identified in a
240 mantle rock.

241 (iii) The two main arguments in favour of syngensis (i.e., morphologic and epitaxial criteria)
242 between diamond and its inclusions are not valid, at least for olivine. Alternative explanations must
243 be provided to demonstrate the growth relationship between diamond and its inclusions.

244 (iv) Other silicate inclusions (e.g., coesite, garnet, pyroxene) in diamond could show an analogous
245 behaviour to that of the olivine.

246 (v) It is important to highlight that we determined the adhesion energies by performing the
247 calculations at $T = 0K$ and $P = 0$. To take into accounts the effect of T and P on the adhesion energy

248 very demanding calculations should be done, which cannot be actually performed with the
249 computational resources at our disposal. Moreover, at the best of our knowledge, there are not
250 works in which the effect of T and P on the energetics of the epitaxial interfaces is discussed. This
251 lack of information prevents to know the behaviour of the adhesion energies when both
252 temperature and pressure increase. To have a realistic estimate of the effect of temperature for the
253 different diamond/forsterite interfaces, it is necessary to determine at *ab initio* level the frequencies
254 of the vibrational modes of the composed slabs, which are essential for calculating the vibrational
255 contribution (i.e., vibrational energy and vibrational entropy) to the interface energy of an epitaxial
256 system (e.g., Bruno, 2015; Bruno and Prencipe, 2013).

257 (vi) We performed the simulations by considering an olivine formed exclusively by the forsterite
258 end-member (Fo_{100}). Nevertheless, typical Earth's mantle olivines contain a small percentage of
259 iron ($\sim\text{Fo}_{92}\text{Fa}_8$), which could affect the values of the adhesion energies. Even in this case there are
260 not estimates of the effect of iron on the interaction between diamond and olivine. There is only a
261 very recent work (Navarro-Ruiz et al., 2014) where the authors calculated at *ab initio* level the
262 surface energy (at 0K and in the vacuum) of the (010) face of Mg-pure (Fo_{100}) and Fe-containing
263 ($\text{Fo}_{75}\text{Fa}_{25}$) olivines. The authors found that the (010) surface energy for $\text{Fo}_{75}\text{Fa}_{25}$ (0.870 J/m^2) is
264 lower by 25% than the (010) surface energy for Fo_{100} (1.160 J/m^2). This means that the iron has
265 certainly a strong effect on the values of the surface energy of the olivine faces and that it is licit to
266 expect that also the adhesion energies could be affected by the presence of fayalite. However, since
267 the mantle olivines are poor in fayalite, it is likely that our estimates of adhesion energy values are
268 only slightly modified by the content of iron. Unless this latter tends to segregate preferentially onto
269 the crystal surfaces of olivine, by increasing the fayalite content at the diamond/olivine interface.
270 Such phenomenon was observed for Ca^{+2} in magnesium silicate olivine rich aggregates by Hiraga et
271 al. (2004) and energetically analysed by Alfredsson et al. (2005) for an orthorhombic MgSiO_3 -
272 perovskite.

273 (vii) Another point to address is the following. We cannot state with absolute certainty that diamond

274 and olivine are in direct contact between them. It should be possible that a very thin layer (a few
275 Ångström thick?) of a fluid (or 2D solid) phase takes place in between diamond and olivine, so
276 forming a more complex interface. Obviously, only the experimental observation on natural samples
277 can give a definitive answer to such a question. It is sure yet that if a similar complex interface
278 exists, then the adhesion energies between diamond and olivine are completely different from those
279 determined in this work. It is for posterity to judge...

280

281 **References**

282 Alfredsson, M., Corà, F., Brodholt, J.P., Parker, S.C., Price, G.D., 2005. Crystal morphology and
283 surface structures of orthorhombic MgSiO₃ in the presence of divalent impurity ions. *Phys.*
284 *Chem. Minerals* 32, 379-387.

285 Becke, A.D., 1993. Density-functional thermochemistry. III. The role of exact exchange. *J. Chem.*
286 *Phys.* 98, 5648-5652.

287 Bruno, M., 2015. The free energy density of a crystal: calcite (CaCO₃) as a case of study.
288 *CrystEngComm*, 17, 2204-2211.

289 Bruno, M., Rubbo, M., Pastero, L., Massaro, F.R., Nestola, F., Aquilano, D., 2015. Computational
290 approach to the study of epitaxy: natural occurrence in diamond/olivine and
291 aragonite/zabuyelite. *Cryst. Growth Des.* 15, 2979-2987.

292 Bruno, M., Massaro, F.R., Prencipe, M., Demichelis, R., De La Pierre, M., Nestola, F., 2014. Ab
293 initio calculations of the main crystal surfaces of forsterite (Mg₂SiO₄): a preliminary study to
294 understand the nature of geochemical processes at the olivine interface. *J. Phys. Chem. C* 118,
295 2498-2506.

296 Bruno, M., Prencipe, M., 2013. A new calculation strategy to analyze the vibrational free energy of
297 a slab and calculate the vibrational contribution of the surface free energy. *CrystEngComm*, 15,
298 6736-6744.

299 De La Pierre, M., Bruno, M., Manfredotti, C., Nestola, F., Prencipe, M., Manfredotti, C., 2014. The

300 (100), (110) and (111) surfaces of diamond: an ab initio B3LYP study. *Mol. Phys.* 112, 1030-
301 1039.

302 Demichelis, R., Bruno, M., Massaro, F.R., Prencipe, M., De La Pierre, M., Nestola, F., 2015. First-
303 principle modelling of forsterite surfaces properties: accuracy of methods and basis sets. *J.*
304 *Comput. Chem.* 36, 1439-1445.

305 Dovesi, R., Saunders, V.R., Roetti, C., Orlando, R., Zicovich-Wilson, C.M., Pascale, F., Civalleri, B.,
306 Doll, K., Harrison, N.M., Bush, I.J., D'Arco, P., Llunell, M., 2009. *CRYSTAL09 User's*
307 *Manual*, University of Torino, Torino, Italy.

308 Dovesi, R., Orlando, R., Civalleri, B., Roetti, C., Saunders, V.R., Zicovich-Wilson, C.M.,
309 2005. *CRYSTAL: a computational tool for the ab initio study of the electronic properties of*
310 *crystals.* *Z. Kristallogr.* 220, 571-573.

311 Frank-Kamenetsky, V.A., 1964. The nature of structural impurities and inclusions in minerals. Gos.
312 Univ., Leningrad. [In Russian].

313 Futergendler, S.I., Frank-Kamenetsky, V.A., 1961. Oriented inclusions of olivine, garnet and
314 chrome-spinel in diamonds. *Zapisky Vsesoyuznogo Mineralogicheskogo Obshchestva* 90, 230-
315 236. [In Russian].

316 Harris, J.W., Gurney, J.J., 1979. In: Field, J.E. (Ed.), *Properties of diamond.* Academic Press,
317 London, pp. 555-591.

318 Harris, J.W., 1968a. The recognition of diamond inclusions. Pt. 1: Syngenetic inclusions. *Industrial*
319 *Diamond Reviews* 28, 402-410.

320 Harris, J.W., 1968b. The recognition of diamond inclusions. Pt. 2: Epigenetic inclusions. *Industrial*
321 *Diamond Reviews* 28, 458-461.

322 Hiraga, T., Anderson, I.M., Kohlstedt, D.L., 2004. Grain boundaries as reservoirs of incompatible
323 elements in the Earth's mantle. *Nature* 427, 699-703.

324 Lee, C., Yang, W., Parr, R.G., 1988. Development of the Colle-Salvetti correlation-energy formula
325 into a functional of the electron density. *Phys. Rev. B* 37, 785-789.

326 Meyer, H.O.A., 1987. In: Nixon, P.H. (Ed.), Mantle xenoliths. John Wiley & Sons, Chichester, pp.
327 501-522.

328 Mitchell, R.S., Giardini, A.A.. 1953. Oriented olivine inclusions in diamond. *Am. Mineral.* 38, 136-
329 138.

330 Mutaftschiev, B., 2001. The Atomistic Nature in Crystal Growth. Springer Series in Materials
331 Science. Springer-Verlag, Berlin, 368 pp.

332 Navarro-Ruiz, J., Ugliengo, P., Rimola, A., Sodupe, M., 2014. B3LYP periodic study of the
333 physiochemical properties of the nonpolar (010) Mg-pure and Fe-containing olivine surfaces. *J.*
334 *Phys. Chem. A* 118, 5866-5875.

335 Nestola, F., Nimis, P., Angel, R.J., Milani, S., Bruno, M., Prencipe, M., Harris, J.W., 2014. Olivine
336 with diamond-imposed morphology included in diamond. Syngenesis or protogenesis?
337 *International Geology Review* 56, 1658-1667.

338 Nestola, F., Nimis, P., Ziberna, L., Longo, M., Marzoli, A., Harris, J.W., Manghnani, M.H.,
339 Fedortchouk, Y., 2011. First crystal-structure determination of olivine in diamond: Composition
340 and implications for provenance in the Earth's mantle. *Earth Planet. Sci. Lett.* 305, 249-255.

341 Neuser, R.D., Schertl, H.-P., Logvinova, A.M., Sobolev, N.V., 2015. An EBSD study of olivine
342 inclusions in Siberian diamonds: evidence for syngenetic growth? *Russian Geology and*
343 *Geophysics* 56, 321-329.

344 Orlov, Y.L., 1977. The mineralogy of the diamond. John Wiley & Sons, New York, 235 pp.
345 [Translation of *Mineralogiiaalmaz, Izdatel'stva Nauka*, 1973, in Russian].

346 Pearson, D.G., Brenker, F.E., Nestola, F., McNeill, J., Nasdala, L., Hutchison, M.T., Matveev, S.,
347 Mather, K., Silversmit, G., Schmitz, S., Vekemans, B., Vincze, L., 2014. Hydrous mantle
348 transition zone indicated by ringwoodite included within diamond. *Nature* 507, 221-224.

349 Pearson, D.G., Shirey, S.B., 1999. In: Lambert, D.D., Ruiz, J.(Eds.), Application of radiogenic
350 isotopes to ore deposit research and exploration. Society of Economic Geologists, Boulder,
351 Colorado, pp. 143-171.

- 352 Pisani, C., Dovesi, R., Roetti, C., 1988. Hartree-Fock ab-initio treatment of crystalline systems.
353 Lecture Notes in Chemistry. Springer-Verlag, Berlin, 195 pp.
- 354 Shirey, S.B., Cartigny, P., Frost, D.J., Keshav, S., Nestola, F., Nimis, P., Pearson, D.G., Sobolev,
355 N.V., Walter, M.J., 2013. Diamonds and the geology of mantle carbon. *Rev. Min. Geochem.* 75,
356 355-421.
- 357 Sobolev, N.V., 1977. Deep-seated inclusions in kimberlites and the problem of the composition of
358 the upper mantle. American Geophysical Union, Washington, D.C., 279 pp.
- 359 Stachel, T., Harris, J.W., 2008. The origin of cratonic diamonds-constraints from mineral inclusions.
360 *Ore Geol. Rev.* 34, 5–32.
- 361 Stephens, P.J., Devlin, F.J., Chabalowski, C.F., Frisch, M.J., 1994. Ab initio calculation of
362 vibrational absorption and circular dichroism spectra using density functional force fields. *J.*
363 *Phys. Chem.* 98, 11623-11627.
- 364 Taylor, L.A., Anand, M., Promprated, P., 2003. Diamonds and their inclusions: are the criteria for
365 syngeneis valid? Eighth International Kimberlite Conference, Extended Abstract, Victoria,
366 Canada, 1-5.
- 367 Taylor, L.A., Anand, M., 2004. The origin of diamonds: time capsules from the Siberian Mantle,
368 2004. *Chem. Erde* 64, 1-74.

369

370 **Acknowledgments**

371 The work was supported by the European Research Council Starting Grant 2012 under grant
372 agreement 307322 to F. Nestola (project INDIMEDEA; www.indimedea.eu). Thanks are due to J.P.
373 Brodholt, G. Pearson and an anonymous reviewer for their careful reading of the manuscript and
374 their fundamental observations on our work.

375